

Imaging System



for Protein Crystallography

- High-resolution structures of biological macromolecules are essential for understanding diseases at molecular level
- The Protein Crystallization Imaging System helps monitor the progress of protein crystal growth during crystallization process
- Multi-focus images of protein crystals in multiple wells are captured by Imaging system

High-resolution structures of the biological macromolecules such as protein, DNA, RNA or their complexes are indispensable for understanding human disease pathways at the molecular level. This understanding is very important for rational drug design. Growth of single crystals of the biological macromolecules is often a bottleneck for macromolecular structure determination. It is difficult for researchers to predict exact conditions for formation of single crystals. Therefore, numerous crystallization trials are often required for a successful crystallization of biological macromolecules. Crystallization trials involve two important steps: a) Setting up the crystallization drops (typical volume 2 micro-litre) in 24 or 96 well plates by mixing equal volume of crystallization condition and solution of biological macromolecules; the setups are carried out using three different methods: hanging-drop, sitting-drop and under-oil microbatch. b) Monitoring crystallization drops during frequent intervals of time for checking the appearance of the single crystals. Various commercial systems have been developed for automation of the first step of the crystallization process [1]. While some limited automation systems are also available for monitoring the second step of the crystallization. All those automation systems are non-indigenous and maintenance of those systems is often costly and cumbersome. There are more than 100 research groups in India which use protein crystallography as a main technique for their structure determinations. Maintaining the records during second step of the crystallization process is often important for the reproduction of the successful crystallization trial which can be very well carried out by automation process. Due to non-availability of the affordable automated systems, the second step is often carried out manually in most of the laboratories. Moreover, some of the biological macromolecules are virus particles or toxic proteins which need to be handled by the automation system without human intervention for the bio-safety reasons. In view of these, we have designed and developed an indigenous protein crystallization imaging system for monitoring the growth of the single crystals, which deals with tasks of well control, image acquisition and analysis. Fig.1 depicts our developed protein crystallization imaging system (PCIS). Lysozyme protein crystals were grown using hanging drop, sitting drop and under-oil microbatch methods of crystallization. The crystal images from those drops as captured by PCIS are shown in Fig.2.

Image processing techniques are used to process the crystal images. Image segmentation and thresholding may help in determining the phase of crystallization. Useful distinguish features like high intensity, sharp boundaries can be extracted from segmented output. But usually due to noise or focusing issues, segmentation may not provide the expected output. Moreover, crystals inside a well are at a different depth of field. Therefore, multiple images of a single well at different depths are captured. Segmentation may be applied on each of these individual images or on a single focused stacked image.

Multiple focus depth images can be combined to form a single focus stack image to visualize all the crystals of well in a single image. Focus stacking is achieved by fusing different in-focus features from multi-depth images [2]. Features extracted with segmentation and thresholding may be used to classify the images into different categories of crystallization process (crystal, clear, precipitate etc.) [3]. A visualization of morphologically good quality crystals by imaging system is essential tool for protein crystallography.

We have developed a complete pipeline from well images capturing to image analysis to retrieval and storage. This paper is structured as follows. Section II elaborates the hardware and design features of the developed system. In Section III, different image analysis algorithm implemented for image fusion and filtering are discussed. In Section IV, software features are discussed.

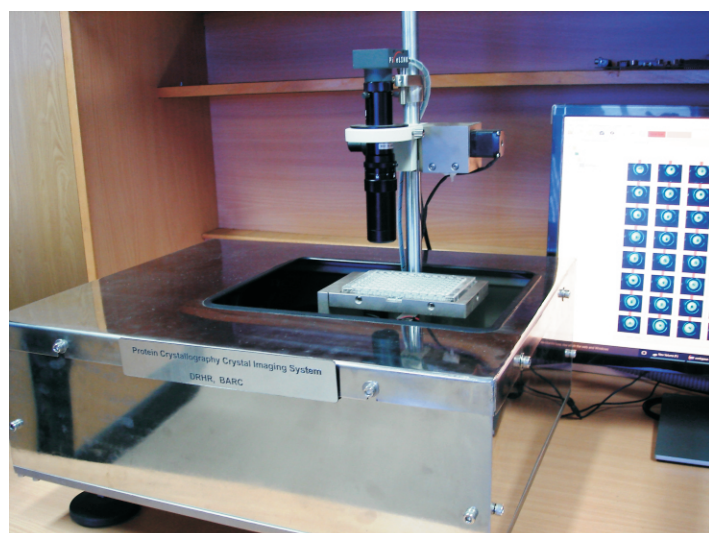


Fig. 1: Protein crystallization Imaging System (PCIS).

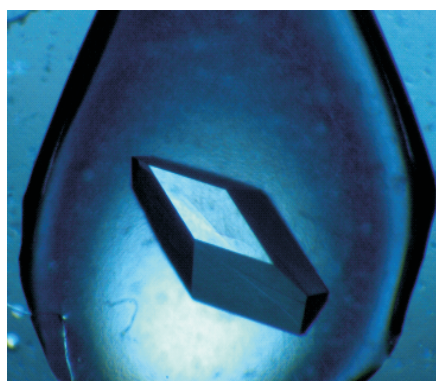
This article was contributed by

¹Ratnesh S. Sengar*, ²Rohit Sharma, ³Ravindra D. Makde

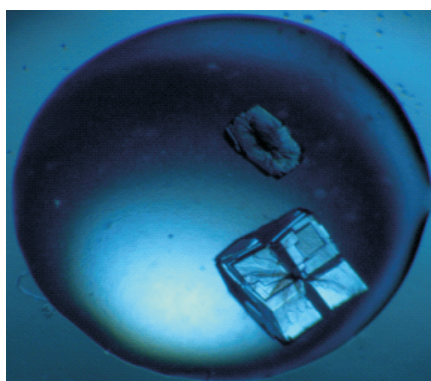
^{1,2}Division of Remote Handling & Robotics, BARC

³Beamline Development & Application Section, BARC

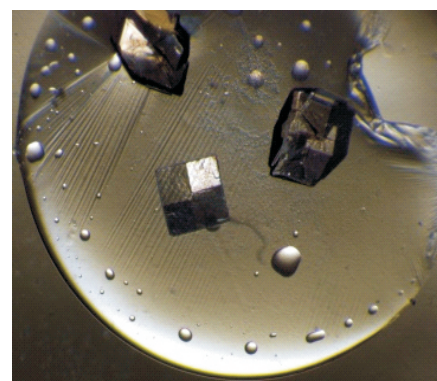
*Corresponding Author email: rssidengar@barc.gov.in



Crystal Image I



Crystal Image II



Crystal Image III

Fig.2: Crystallization drops as captured by PCIS.

The monitoring of microscopic size of crystals in 24/96 well by robotic imaging system demands very high accuracy. Various design considerations and the quality parameters to be accessed while monitoring crystals are also discussed in subsequent sections.

Hardware and design features

The important considerations while designing a precise imaging system for crystal monitoring are: a) micron level motion accuracy at a scale of 120mmx 120mm x 50mm with minimum vibration and b) automatic acquisition and visualization of multi-focal images of macromolecular protein crystals in standard multi-well crystallization plate. We achieved this by using a well damped table, grounded linear guides, servo motors with absolute encoders and custom designed high-resolution microscopic imaging system with image processing algorithms. The entire assembly is precisely leveled, while the frame structure below the table is utilized to hold the control panel. Typical setup for a crystallization imaging system involves number of components which are as follows:

a) *High resolution microscopic imaging system:* A camera and zoom lens is mounted on rack and pinion mount. Motor is coupled with rack and pinion mount to capture multi-focus images at different depth of a drop with different magnifications. A limit switch is placed on top of rack pinion mount for homing of imaging system which helps to calibrate the image and auto focusing of each well of crystallization plate.

b) *Customized illumination control to locate the drop:* 100% diffused light source with collimated optics is designed to focus all the crystallization drops without reflection.

c) *Robotic stages:* The robotic stage has a motion travel of 120mmx120mm in X and Y directions. A grounded linear guide is used to reduce the backlash error in each axis. A compact servo motor with absolute encoder is used for precise motion.

d) *Plate handler:* It holds standard crystallization plates of 24/96/384 wells. Inside the boundary of

plate handler switch locator is provided to avoid the movement in the plate and precisely locate the drop in each well by illuminator.

e) *Control system for robotic stages and microscopic imaging system:* A realistic dynamic model of the robotic system is constructed [4] and tuned for stable operation in each axis. The position, speed and current loop compensators are implemented as software-based lead, lag compensator and notch filter. The corresponding bandwidth is achieved in position loop 40Hz, speed loop 100hz and current loop 1200Hz.

Image processing and feature extraction

Imaging of the crystallization drops in multi-well plate is challenging due to following reasons:

- ◆ Images may be captured under different illumination; therefore, global threshold segmentation algorithms do not work on these images [1].
- ◆ Crystals may appear at different depth of field in crystallization drop (typical drop volume of 2 microlitre) and entire drop cannot be focus at the same time due to optical limit of cylindrical zoom lens. Hence, auto-focus and real time image fusion algorithms are required on multi-focus images to maximise the depth of field.
- ◆ Sizes and number of crystals vary in a particular crystallization drop. Different Images captured at different phases of crystal growth may have varying shape and intensities. This poses a challenge in crystal classification.

These above challenges posed by protein crystal imaging lead us to propose different imaging steps and image classification methods. Each method provides different insights into the problem and significant improvements in the crystallization methods. Image segmentation plays a big role in image classification to find out the robust features for training the classification model.

Image segmentation plays a big role in image classification to find out the robust features for training the classification model

Image denoising

Protein crystal images contain features that are about 10-300 microns in size and having sharp boundaries. Sometimes, non-linear background and noise makes it difficult to extract the features from crystal images. Therefore, prior to feature extraction, image filtering is applied to remove noise from the image [1]. Traditional denoising techniques like Box filter, fourier transform, wavelet transform fail to denoise the crystal image. Either the image is blurred or sharp features are smoothed out. We compared different denoising algorithms in spatial as well as transform domain and found that for denoising of protein crystal images, anisotropic diffusion median (AMD) [6] results better in terms of SNR as well as in universal quality index.

Perona and Malik [5] anisotropic diffusion equation for noisy image I is given in below equation.

$$I_t = \text{div}(c(x, y, t)\nabla I) = c(x, y, t)\Delta I + \nabla c \cdot \nabla I \quad (1)$$

where div is the divergence operator, Δ is the Laplacian operator and ∇ is the gradient operator and $c(x, y, t)$ is diffusivity function. Anisotropic diffusion median (AMD)[6] incorporates a median filter into a diffusion step and works as a hybrid filter that achieves much better noise suppression with minimum edge blurring than any other diffusion algorithms. Diffusivity function for AMD is chosen as Tukey biweight function [9]. Tukey biweight function is given in below equation.

$$c(\nabla I, K) = \begin{cases} \frac{25}{16K} \left[1 - \left(\frac{|\nabla I|}{\sqrt{5}K} \right)^2 \right]^2, & |\nabla I| \leq \sqrt{5}K \\ 0 & \text{otherwise} \end{cases} \quad (2)$$

Where K acts as threshold and is constant as is tuned for particular application.

$$I_{i,j}^{n+1} = \text{Median}(I_{i,j}^{n+1}, W) \quad (3)$$

W is the window for median operator. This diffusion algorithm converges in a smaller number of steps, thus makes it suitable for real time implementation.

The best SNR achieved on protein crystal images by diffusion methods, resulted in an improvement in feature extraction of crystals and classification of crystallization trails.

Feature extraction using image segmentation

Image thresholding techniques aid the segmentation algorithm by converting the image to binary image. Global thresholding works by maximizing the variance between the classes.

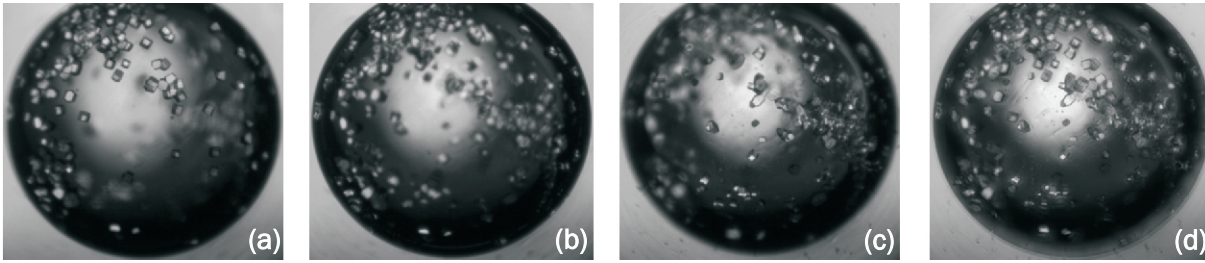
Ostu [7] technique works by finding the optimal threshold. But this is not always possible to find the distinctive peaks. Unlike global thresholding, local thresholding [1] works by analysing the features in local neighbourhood of image. This leads to increase in complexity and for poor illuminated images local thresholding may incorrectly classify background and foreground pixels. Gradient based image segmentation may give inaccurate results in poorly illuminated images. Region-based segmentation combines similar pixels by region growing and gives promising results. Usually, region-based segmentation may involve user intervention e.g. by providing markers and may not be suitable for automated crystal image segmentation. Wavelet based image segmentation is a multi-resolution transform domain image segmentation technique which first decompose the image into high pass and low pass coefficients. Wavelets have limited frequency support and find features only in limited directions. We have implemented a contourlet-based multiresolution, multidirectional segmentation algorithm [8] to extract various features associated with crystals.

Image fusion or focus stacking

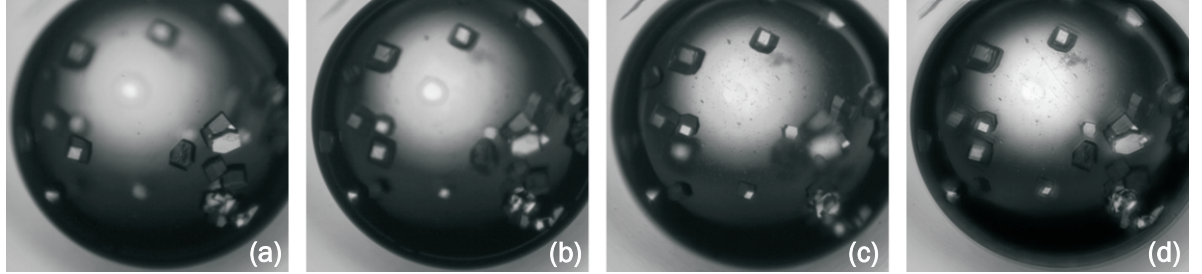
In-focus features extracted from segmentation algorithm of multi-depth images needed to be fused together to form a single composite fused image. Pixel based fusion algorithms uses maximum selection criteria by comparing the pixel values of all images and selects the maximum one.

Neighbourhood based fusion algorithms are based on utilizing the neighbourhood pixels within a fixed window [2]. Froster et al. proposed a complex wavelet transform based image fusion algorithm. Multiscale image fusion [2][10], data driven image fusion give better results but might leads to brightness distortions. A guided filter fusion [9] (GFF) method based on guided filtering is computationally efficient and can be used in real time applications but this algorithm also leads to brightness and contrast distortions. To overcome these limitations, we have proposed a fusion algorithm with combination of non-subsampled wavelet transform (NSWT) and guided filter.

A contourlet-based multi-resolution, multi-directional segmentation algorithm was implemented to extract various features associated with crystals



(i) Images (a-c) captured with different depths of focus and (d) is final fused image.



(ii) Images (a-c) captured with different depths of focus and (d) is final fused image.

Fig.3: Fusion algorithm results for two wells images captured with different depth of focus.

Our Proposed algorithm

The source input images are first decomposed using forward non subsampled wavelet transform (NSWT) [8]. Input image is decomposed to an approximation image and detail directional images using directional filter banks (DFBs). The discrete NSWT of source image $I(x,y)$ of size $M \times N$ is given by:

$$W_{\Phi}^k(j_o, m, n) = \frac{1}{\sqrt{MN}} \sum_{x=0}^{M-1} \sum_{y=0}^{N-1} I^k(x, y) \Phi_{j_o, m, n}(x, y) \quad (4)$$

$$W_{\Psi}^{k,i}(j_o, m, n) = \frac{1}{\sqrt{MN}} \sum_{x=0}^{M-1} \sum_{y=0}^{N-1} I^k(x, y) \psi_{j_o, m, n}^i(x, y), \quad i = \{H, V, D, \dots\} \text{ and } j \geq j_o \quad (5)$$

$I^k(x, y)$ is k^{th} source image and $W_{\Phi}^k(j_o, m, n), W_{\Psi}^{k,i}(j_o, m, n)$ are approximation and details coefficients for direction $i = \{H, V, D, \dots\}$ respectively. j_o is starting scale and Φ, Ψ are scaling and wavelet function respectively. H, V, D are horizontal, vertical and diagonal directions respectively. Weight map is constructed by performing guided filtering on each bandpass image with source image as a guidance image.

$$W_B^k = G_{r_1, \epsilon_1}(W_{\Phi}^k, I^k) \quad , \quad W_D^{k,i} = G_{r_2, \epsilon_2}(W_{\Psi}^{k,i}, I^k) \quad (6)$$

$r_1, \epsilon_1, r_2, \epsilon_2$ are parameters of guided filter G and are determined empirically. W_B^k and $W_D^{k,i}$ are refined weights of approximation and detail coefficients respectively and these weights are normalized. Approximation and details coefficients of different input images are fused together by weighted averaging.

$$\overline{W_{\Phi}^k(j_o, m, n)} = \sum_{k=1}^K W_B^k W_{\Phi}^k(j_o, m, n) \quad , \quad \overline{W_{\Psi}^{k,i}(j_o, m, n)} = \sum_{k=1}^K W_D^{k,i} W_{\Psi}^{k,i}(j_o, m, n) \quad (7)$$

Then, final fused image $F(x,y)$ is found by applying inverse NSWT (INSWT) to refined coefficients $\overline{W_{\Phi}^k(j_o, m, n)}$ & $\overline{W_{\Psi}^{k,i}(j_o, m, n)}$

$$F(x, y) = \frac{1}{\sqrt{MN}} \sum_m \sum_n \overline{W_{\Phi}^k(j_o, m, n)} \Phi_{j_o, m, n}(x, y) + \frac{1}{\sqrt{MN}} \sum_{i=H,V,D} \sum_{j=j_o}^{\infty} \sum_m \sum_n \overline{W_{\Psi}^{k,i}(j_o, m, n)} \psi_{j_o, m, n}^i(x, y) \quad (8)$$

Experiments were performed on multiple images captured by our system and we have found that our proposed algorithm works better than other existing algorithms like Focus All [2], GFF [9], HOSVD [10], NSCT on the basis of quality index. Fused image output from our proposed algorithm is shown in Fig.3.

Crystal size measurement

Actual crystal shape and size can aid researchers to analyse the crystal quality for X-ray diffraction studies. Physical size calculation is not a trivial task and is limited by zoom-lens and focus setting. Existing zoom-lens calibration methods usually employ precisely measured targets as ground truth. Fraser and Al Ajlouni [11] used a 3D control field for zoom-lens calibration comprised of a 140 object point array covering an area of about $5m \times 3m$. In close-range computer vision applications using zoom-lens cameras, the lens and focus settings are subject to frequent changes, and this leads to frequent calibration which is not feasible and inefficient.

We have developed a flexible method to calibrate a zoom-lens camera. We have used a NIST certified calibration target

Actual crystal shape and size can aid researchers to analyse the crystal quality for X-ray diffraction studies.

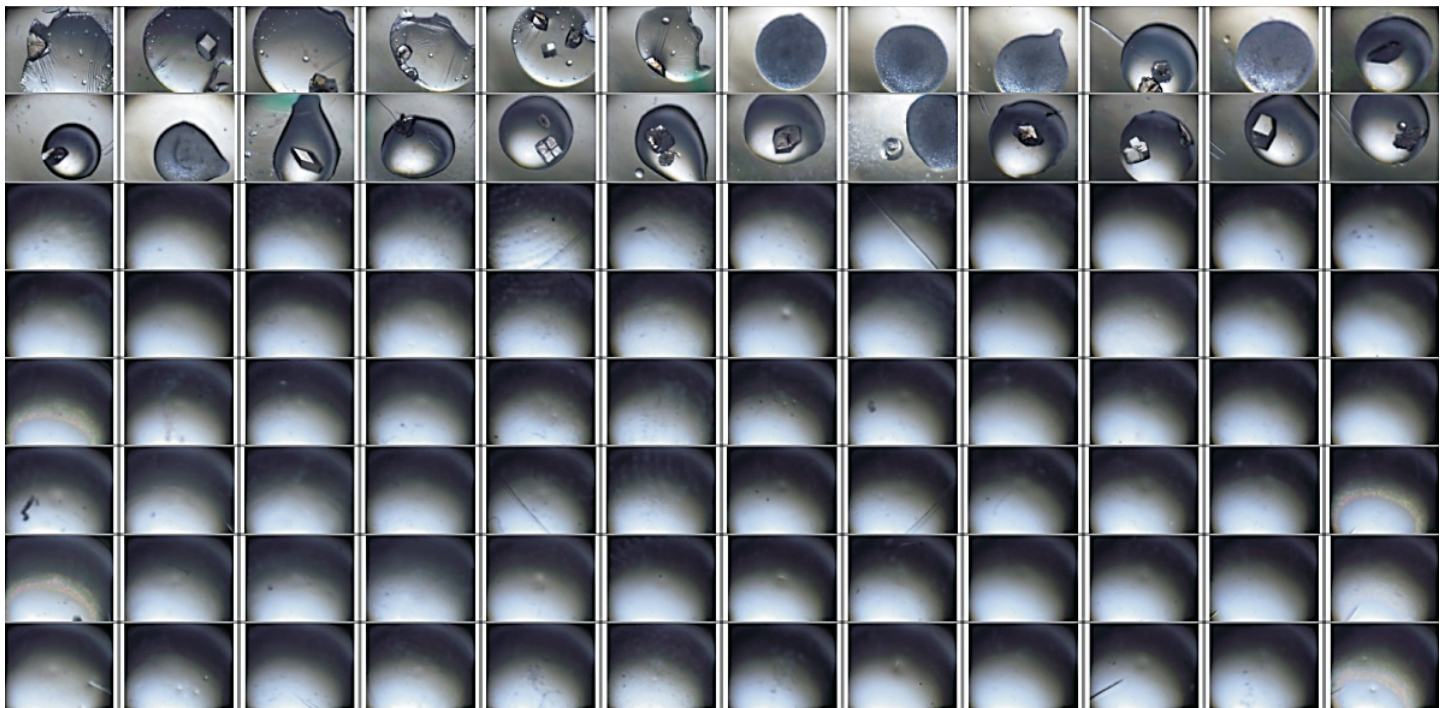


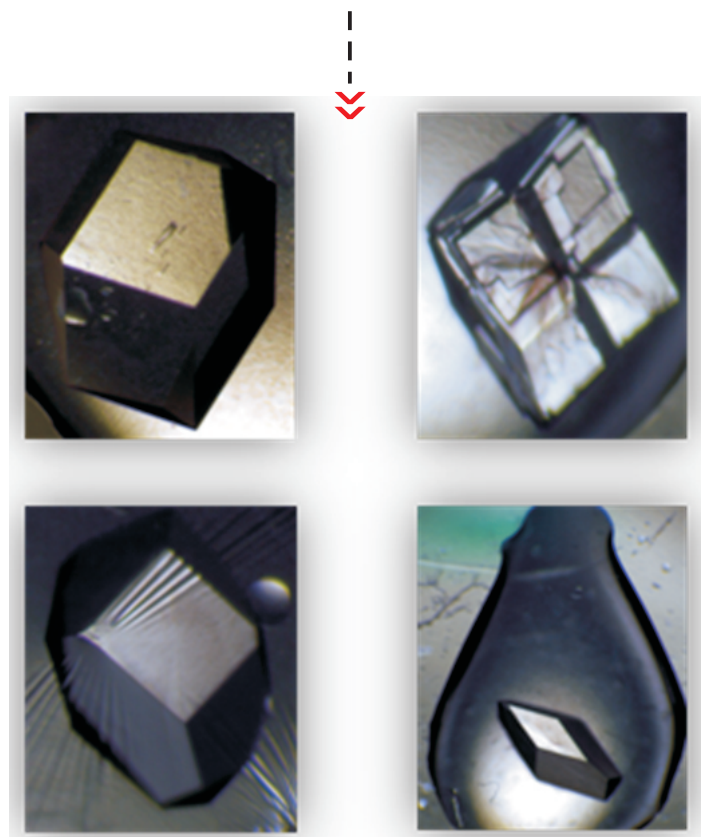
Fig.4: Crystallography software graphical user interface.

to calibrate zoom camera. First, multiple images of calibration target at different zooms and different heights are captured. A physical to pixel coordinates mapping is calculated. A multivariable linear regression model has been built using this data. Model coefficients are saved to a configuration file. Real time crystal size is estimated using these model coefficients. Accuracy of this model is established by comparing the actual size and calculated size. The error is less than 10 microns.

Protein crystallography imaging software

User friendly, intuitive, multithreaded, modular, robust, control and analysis software is developed by incorporating all the algorithms discussed in the previous sections. The software is developed by keeping in view the best practises followed in industry. Software main graphical user interface is shown in Fig.4.

Some of the features of software are given below (crystal vision software). Software provides seamless integration with hardware. Automatic scheduling is managed through the software. User can inspect the crystals in a well plate at any time by manual controls provided in the software. User can fine tune settings to improve the imaging accuracy. Once, control module has captured images. These images can be viewed in an image view.



CRYSTAL VISION SOFTWARE - FEATURES

Control	Analysis	GUI
Robotic control	Autofocus algorithm	Workspace management (Project and experiment)
Well configuration and calibration	Feature extraction	Image viewing and comparison mode (canvas, well, drop)
Camera control	Image fusion	Image storage and retrieval
Manual movement module	Crystal classification	Job scheduler

Conclusion

The protein crystal imaging system (PCIS) is an attempt to indigenously develop high throughput system for monitoring the crystal growth in crystallization drops during the crystallization process. This facilitates the research using x-ray crystallography in the area of structural biology and rational drug discovery. Here, we described the design and implementation of standalone real-time, affordable system for protein crystallization image acquisition. High resolution imaging system coupled with diffused illumination light source and robotic stages provides support for imaging of a single wellplate of customizable configurations. Images at different depth for each well at different intervals of time are captured and stored in the database. Image analysis is carried out on crystal images. Comparison of different denoising algorithms yields the anisotropic diffusion-based algorithm the right choice for the crystal images. Focus stacked images of each well are fused together by powerful, fast and efficient NSCT-guided fusion algorithm. Advantage of this algorithm lays in efficiency and minimal brightness distortions. Image acquisition and processing for a 96 well plate take less than 12 minutes, hence greatly reducing manual inspection of the crystallization plate. Correct classification of images into crystals and non-crystals can further reduce the unnecessary inspection of the plate. As future work, we intend to develop a convolutional neural network (CNN) to classify the images into different categories.

Acknowledgments

The authors would like to thank Vinay Kumar, Former Head, RB&HSD and Gagan D Gupta, RB&HSD for providing the protein crystal samples and useful suggestions for validating the system. We also thank to Amit Das, RB&HSD for valuable discussion at various stages of this project. We would also like to show our gratitude to K Madhusoodnan Head, DRHR for the support and encouragement during the course of this indigenous development. We are grateful to D.C. Kar, Head, Medical Robotics Section, DRHR for his kind support.

References

- [1] Pusey, Marc & Aygun, Ramazan, "Data Analytics for Protein Crystallization", 2017, 10.1007/978-3-319-58937-4.
- [2] M.S. Sigdel, M. Sigdel, S. Dinç, I. Dinc, M.L. Pusey and R.S. Aygün, "FocusALL: Focal Stacking of Microscopic Images Using Modified Harris Corner Response Measure," in *IEEE/ACM Transactions on Computational Biology and Bioinformatics*, 2016, Vol. **13**, 2, 326-340, doi: 10.1109/TCBB.2015.2459685.
- [3] Bruno, E Andrew *et al.* "Classification of crystallization outcomes using deep convolutional neural networks." *PloS one*, 2018, Vol.**13**, 6e0198883. doi:10.1371/journal.pone.0198883.
- [4] Ogata Katsuhiko, "Modern control system" Prentice Hall, 1992.
- [5] Pietro Perona and Jitendra Malik, "Scale-space and edge detection using anisotropic diffusion" (PDF). *IEEE Transactions on Pattern Analysis and Machine Intelligence*, 1990, Vol.**12**, 7, 629–639. doi:10.1109/34.56205.
- [6] H. Ling and A.C. Bovik, "Smoothing low-SNR molecular images via anisotropic median-diffusion," in *IEEE Transactions on Medical Imaging*, 2002, Vol. **21**, 4, 377-384. doi:10.1109/TMI.2002.1000261.
- [7] N. Otsu, "A Threshold Selection Method from Gray-Level Histograms," in *IEEE Transactions on Systems, Man, and Cybernetics*, 1979, Vol. **9**, 1, 62-66. doi: 10.1109/TSMC.1979.4310076.
- [8] L. da Cunha, Jianping Zhou, and Minh N. Do, "The non subsampled contourlet transform: theory, design, and applications," *IEEE Transactions on Image Processing*, 2006, Vol. **15**, 10, 3089–3101.
- [9] S. Li, X. Kang and J. Hu, "Image Fusion With Guided Filtering," in *IEEE Transactions on Image Processing*, 2013, Vol. **22**, 7, 2864-2875. doi:10.1109/TIP.2013.2244222.
- [10] J. Liang , Y. He , D. Liu , X. Zeng , " Image fusion using higher order singular value decomposition", *IEEE Transactions on Image Processing*, 2012, Vol. **21**, 5, 2898-2909. doi:10.1109/tip.2012.2183140.
- [11] C.S. Fraser, and S. Al-Ajlouni, "Zoom-dependent camera calibration in digital close-range photogrammetry", *Photogrammetric Engineering & Remote Sensing*, 2006, Vol. **72**, 9, 1017–1026.